Research Article

Journal of Labelled Compounds and Radiopharmaceuticals

Received 18 December 2009, Revised 20 January 2010, Accepted 25 January 2010 Published online 30 March 2010 in Wiley Interscience

(www.interscience.wiley.com) DOI: 10.1002/jlcr.1748

Radiosynthesis and *in vivo* evaluation of a F-18-labeled pancreatic islet amyloid inhibitor

Gopal Pathuri, Hrushikesh B. Agashe, Vibhudutta Awasthi, and Hariprasad Gali*

Formation of islet amyloid deposits contributes to the progressive loss of beta-cells in Type 2 diabetes. Islet amyloid is composed of islet amyloid polypeptide (IAPP). [(N-Me)G^{24}, (N-Me)I^{26}]hIAPP(22–27) peptide was found to bind human IAPP with high-affinity and inhibit fibrillogenesis. We labeled [(N-Me)G^{24}, (N-Me)I^{26}]hIAPP(22–27) with fluorine-18 using *N*-succinimidyl-4-[^{18}F]fluorobenzoate. Results from biodistribution studies in healthy CF-1 mice at 1 h p.i. indicated that ^{18}F-peptide was cleared efficiently (0.04 ± 0.02%ID/g remained in blood). The primary route of clearance from the body appears to be hepatobiliary. Radioactivity accumulation in liver, intestine, and kidney was 6.7 ± 2.9, 60.3 ± 18.5, and 0.2 ± 0.0%ID, respectively. Other organs accumulated negligible radioactivity. As normal mice do not develop pancreatic amyloid deposits, only background radioactivity was seen in pancreas. The radio-HPLC analysis of mouse urine at 2 h p.i. showed that ~29.3% of injected ^{18}F-peptide excreted intact along with two additional metabolite peaks. Dynamic microPET/CT imaging of a CF-1 mouse injected with ^{18}F-peptide indicated that radiotracer was rapidly taken up by liver and most of it moved into intestine within 10 min. The results provide a useful insight into the biological disposition of [(N-Me)G^{24}, (N-Me)I^{26}]hIAPP(22–27) that is being developed as a pancreatic amyloid inhibitor.

Keywords: pancreatic islet amyloid; hIAPP(22–27); inhibitor; [^{18}F]SFB; [^{18}F]FBA; PET imaging; F-18-labeled peptide; biodistribution; pharmacokinetics; metabolic stability

Introduction

Several studies suggest that the formation of pancreatic islet amyloid deposits may be a major contributor to the progressive loss of pancreatic beta-cells.[1–4] These deposits are known to be a characteristic pathologic feature of the pancreas in >90% of patients with Type 2 diabetes.[5–6] Pancreatic islet amyloid deposits in humans consist mainly of β sheet fibrillar aggregates of the 37-amino acid islet amyloid polypeptide (IAPP or amylin).[4,5,7] IAPP is a neuroendocrine hormone of the calcitonin family of polypeptide hormones, and is produced and co-secreted with insulin in response to beta-cell stimulation by both glucose and non-glucose secretagogues.[8] IAPP is over-produced in states of insulin resistance, a typical feature of Type 2 diabetes. Excess IAPP promotes self-aggregation and amyloid fibril formation that are thought to be toxic to beta-cells.[4] That islet amyloidosis is an early factor responsible for beta-cell failure is strongly supported by the *in vitro* cytotoxic effect of human islet amyloid polypeptide (hIAPP), as well as by the results from *in vivo* hIAPP transgenic mouse studies.[9,10] The precise mechanisms by which hIAPP-derived fibrils induce beta-cell death and dysfunction are still not clear. It has been suggested that the presence of hIAPP fibrils between islet cells and capillary endothelial cells may impair movement of nutrients (such as glucose) from the bloodstream into beta-cells. At the same time, insulin exocytosed by beta-cells also faces this barrier before reaching the circulation.[11,12] Another proposed mechanism is that these fibrils form pores in the membrane that allows extracellular calcium to enter the cell resulting in apoptotic cell death.[13,14] However, recently it has been suggested that prefibrillar aggregates (or oligomers) formed early during aggregation, and not mature amyloid fibrils, are the cytotoxic species in Type 2 diabetes.[15,16]

Although the sequence of IAPP is strongly conserved over a number of animal species, IAPP-derived amyloid is only formed by humans, cats, and few non-human primates.[17] Rodents do not form pancreatic amyloid, although rat IAPP sequence differs from its human analog by only six amino acid residues. Considering that five of these six amino acid residues are located between residues 20 and 29, amyloidogenicity of hIAPP has been related to these residues. It has been shown that the synthetic decapeptide hIAPP(20–29) is able to form fibrils with morphology that is similar to the fibrils formed by the complete hIAPP sequence.[18] The 'amyloid core' has been further narrowed down to the residues 22–27 (NFGAIL) that has been shown to

Small Animal Imaging Facility, Department of Pharmaceutical Sciences, The University of Oklahoma College of Pharmacy, Oklahoma City, OK 73117, USA

**Correspondence to: Hariprasad Gali, The University of Oklahoma College of Pharmacy, 1110 N. Stonewall Avenue, Room 301, Oklahoma City, OK 73117, USA.*
E-mail: hgali@ouhsc.edu

participate in hIAPP self-association into â-sheets and amyloid fibril formation.[19]

Compounds that block cytotoxic protein/polypeptide self-assembly and amyloidogenesis or fibril formation are therefore important targets for use in therapeutic intervention.[20,21] There are two classes of hIAPP amyloidogenicity and/or cytotoxicity inhibitors: (1) aromatic organic compounds such as Congo red, rifampicin, and others that bind to amyloid fibrils and/or suppress amyloid-fibril formation,[4,22] and (2) short synthetic peptides derived from hIAPP sequences that contain hIAPP self-recognition domains.[23] The synthetic peptides suffer from a disadvantage of being able to undergo self-amyloidosis, which limits their application in therapeutics development. A few modifications in the NFGAIL sequence have been able to overcome self-amyloidosis without altering their inhibitory effect on hIAPP fibrillogenesis. For instance, NFGAIL has been converted into a non-amyloidogenic and non-cytotoxic sequence by N-methylation at Gly^{24} and $Ile.^{24,25}$ The strategy of N-methylation of peptide amide bonds has been a well-known protein-design approach to suppress H-bonding ability of an >NH group and to restrict the conformation of the backbone. The N-methylated analog, [(N-Me)G^{24}, (N-Me)I^{26}]hIAPP(22–27), conjugated with 5(6)-carboxyfluorescein on the N-terminus has been found to selectively bind hIAPP *in vitro* as well as *in vivo*-formed human pancreatic islet amyloid deposits in human pancreatic tissue obtained postmortem.[24,25]

Here we report radiosynthesis and preliminary *in vivo* evaluation of F-18-labeled [(N-Me)G^{24}, (N-Me)I^{26}]hIAPP(22–27) peptide in normal mice. The overall goal of this study was to explore the possibility of using the pancreatic amyloid inhibitor as a targeting vector for *in vivo* imaging of pancreatic islet amyloid deposits using positron emission tomography (PET). Non-invasive assessment of islet amyloid deposits would provide an important tool for both monitoring therapeutic interventions and better understanding of the natural history of the disease.

Results and discussion

We have selected [(N-Me)G^{24}, (N-Me)I^{26}]hIAPP(22–27) peptide based on its documented ability to selectively bind to hIAPP *in vitro* ($K_d = 129 \pm 59$ nM), as well as to the *in vivo*-formed human pancreatic islet amyloid deposits in human pancreatic tissue obtained postmortem.[24,25] The goal of this study was to evaluate its biodistribution and clearance properties by radiolabeling with ^{18}F and following it *in vivo* by PET imaging.

We labeled [(N-Me)G^{24}, (N-Me)I^{26}]hIAPP(22–27) with fluorine-18 using a [^{18}F]SFB prosthetic group. [^{18}F]SFB was synthesized as shown in Figure 1 by slight modifications in the published procedure.[26,27] The non-radioactive analog, FB-[(N-Me)G^{24}, (N-Me)I^{26}]hIAPP(22–27), was synthesized by reacting the peptide with SFB in presence of triethylamine. It was purified by HPLC and characterized by electrospray mass spectrometry. It was used as a non-radioactive reference for characterizing [^{18}F]FB-[(N-Me)G^{24}, (N-Me)I^{26}]hIAPP(22-27)(^{18}F-peptide) using HPLC. The conjugation reaction of [^{18}F]SFB and peptide was carried out in presence of triethylamine at 90°C for 35 min.

As shown in Figure 2, the HPLC retention times of [^{18}F]SFB and ^{18}F-peptide were very close (11.3 min versus 10.9 min, respectively under identical HPLC conditions). To overcome the separation problem and obtain pure ^{18}F-peptide for animal studies, we added 1 M NaOH to the reaction mixture after conjugation to completely hydrolyze the unreacted [^{18}F]SFB. The [^{18}F]FBA, hydrolysis product of [^{18}F]SFB is relatively more hydrophilic than the precursor [^{18}F]SFB (9.8 min versus 11.3 min,

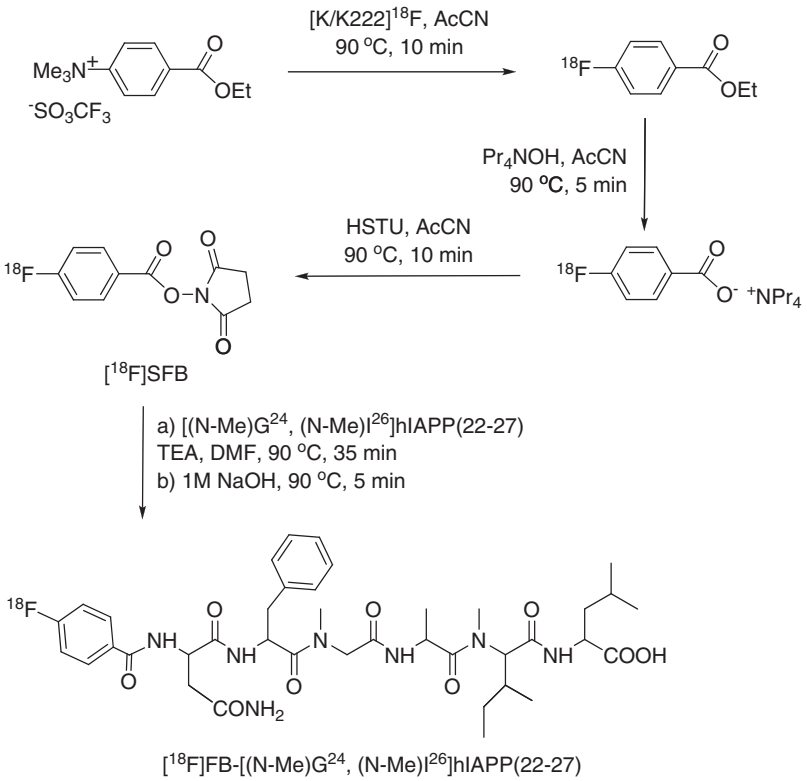

Figure 1. Radiosynthesis of [^{18}F]FB-[(N-Me)G^{24}, (N-Me)I^{26}]hIAPP(22–27).

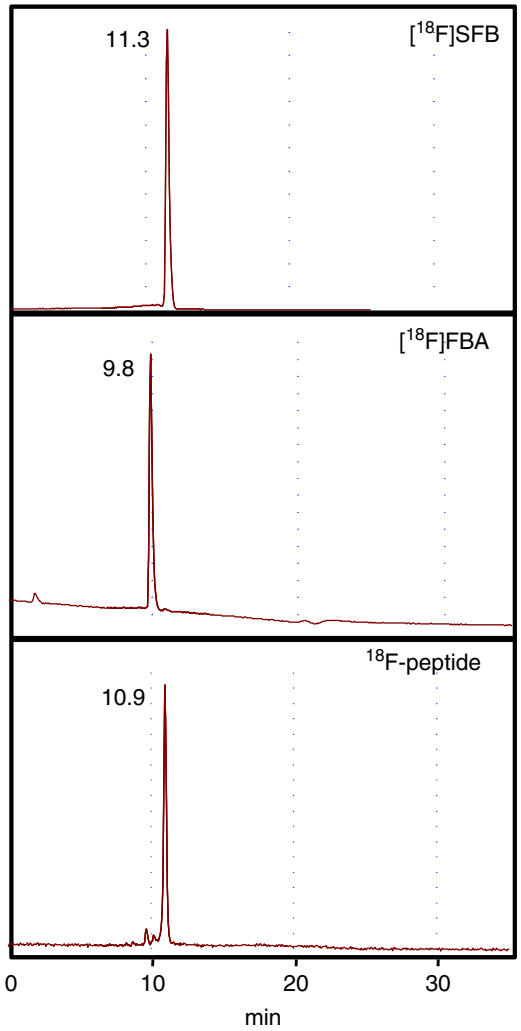

Figure 2. Radio-HPLC chromatograms.

respectively, under identical HPLC conditions) and can be easily separated from ^{18}F-peptide on HPLC.

Results from *in vivo* biodistribution studies of ^{18}F-peptide performed on healthy CF-1 mice at 1 h p.i. are summarized in Table 1. The ^{18}F-peptide was found to be cleared efficiently from blood. Only ~0.04%ID/g remained in blood at 1 h p.i. The primary route of radioactivity clearance from the body appears to be hepatobiliary. About 60.3 ± 18.5%ID accumulated in intestine, whereas liver-associated radioactivity was found to be 6.7 ± 2.9%ID at 1 h p.i. The retention of radioactivity in kidneys (0.22 ± 0.04%ID/g at 1 h p.i.) was found to be lower than that shown for most other small peptide radiopharmaceuticals.[28] Other organs accumulated negligible radioactivity.

The radio-HPLC analysis of the mouse urine collected at 2 h p.i. of ^{18}F-peptide showed that ~29.3% (3rd peak) of the radioactivity was excreted intact; however, two additional metabolite peaks were observed (Figure 3). One of the metabolite (~42.3%, 2nd peak) was identified as *para*-[^{18}F]fluorohippurate ([^{18}F]PFH). Non-radioactive PFH was synthesized and used as an HPLC reference for characterizing [^{18}F]PFH. Literature search showed that [^{18}F]PFH is an expected product from glycine conjugation reaction of [^{18}F]FBA in liver.[29,30] Conjugation with glycine is an important mechanism for elimination and detoxification of several xenobiotic and endogenous carboxylic acids such as benzoic acids.[31] The conjugation reaction is a multi-step process that takes place in the mitochondrial matrix and catalyzed by two enzymes, benzoyl-coenzyme A synthetase and glycine *N*-acyltransferase.[32] Thus, we speculate that [^{18}F]FBA is also metabolized in the same fashion as other benzoic acid derivatives in liver. Although not proven, we hypothesize that [^{18}F]FBA is formed *in vivo* after metabolic cleavage of the C-terminal amide bond of ^{18}F-peptide. The other more hydrophilic metabolite (1st peak) may be the product obtained from metabolic cleavage of the amide bond between asparagine and phenylalanine. The *in vivo* metabolic stability of this peptide was found to be higher than other small linear peptide radiopharmaceuticals, probably due to N-methylation of glycine and isoleucine.[33] This high metabolic stability is a critical aspect for its therapeutic use to inhibit pancreatic amyloid formation.

As the retention time of ^{18}F-peptide was very close to that of [^{18}F]SFB, we also performed biodistribution studies of [^{18}F]SFB in healthy CF-1 mice to confirm that the results obtained with ^{18}F-peptide are not due to the presence of [^{18}F]SFB in the injected dose. We also performed biodistribution studies of the expected ^{18}F-peptide metabolite, [^{18}F]FBA, in healthy CF-1 mice to see its influence on the overall biodistribution profile attributed to ^{18}F-peptide.

As seen in Table 1, the biodistribution profile of [^{18}F]SFB and [^{18}F]FBA were entirely different from that observed for the ^{18}F-peptide. Both [^{18}F]SFB and [^{18}F]FBA cleared from blood primarily through renal/urinary pathway. Only 1.19 ± 0.16%ID and 0.44 ± 0.25%ID remained in intestine for [^{18}F]SFB and [^{18}F]FBA respectively at 1 h p.i. The blood clearance of [^{18}F]FBA was significantly faster than that of [^{18}F]SFB. At 1 h p.i., 5.05 ± 0.46%ID of [^{18}F]SFB remained in blood whereas only 0.07 ± 0.03% [^{18}F]FBA was seen after 1 h. Accumulation of radioactivity in other tissues was significantly lower with [^{18}F]FBA than that of [^{18}F]SFB. The HPLC analysis (Figure 3) of the mouse urine at 30 min p.i. of [^{18}F]FBA showed that it was completely metabolized into [^{18}F]PFH and other more hydrophilic (unknown) products. No formation of the [^{18}F]PFH metabolite was observed with [^{18}F]SFB. We believe that [^{18}F]SFB may be able to bind to the plasma protein before being taken up by liver. As [^{18}F]SFB is an active ester, it may react with the free primary amine groups present on the plasma protein. The physiological pH is suitable for this reaction. The high radioactivity seen in blood with [^{18}F]SFB may be due to the protein binding. More studies are needed to confirm this conjecture.

As the biodistribution profile and clearance pathways of ^{18}F-peptide, [^{18}F]SFB, and [^{18}F]FBA were found to be significantly different, it is clear that ^{18}F-peptide dose injected into mice was radiochemically pure and does not contain any unreacted [^{18}F]SFB. Hydrolysis of unreacted [^{18}F]SFB prior to HPLC purification of the F-18-labeled peptide appears to be a good choice if HPLC retention times of both [^{18}F]SFB and F-18-labeled peptide are very close.

The small animal PET/CT imaging study of ^{18}F-peptide performed on a healthy CF-1 mouse (Figure 4) indicated that the peptide is rapidly taken up by liver. As shown in Figure 4, liver was found to accumulate large amounts of radioactivity within the first 1 min p.i.; most of this radioactivity moved into intestines by 10 min p.i. At 60 min p.i., the radioactivity signal only originated from liver and intestine, which confirms the result of the biodistribution study at 1 h p.i. High uptake of radioactivity by liver and intestine will hinder the visibility of the pancreatic uptake (in presence of amyloid fibrils) in a PET image

Table 1. Biodistribution (%ID/g tissue) of ^{18}F-peptide, [^{18}F]SFB, and [^{18}F]FBA in healthy CF-1 mice at 1 h p.i

Organs	^{18}F-peptide		[^{18}F]SFB		[^{18}F]FBA	
	%ID/g tissue	%ID/organ	%ID/g tissue	%ID/organ	%ID/g tissue	%ID/organ
Blood	0.04 (0.02)	0.10 (0.05)	3.7 (0.3)	5.7 (0.7)	0.05 (0.03)	0.07 (0.03)
Heart	0.04 (0.02)	0.01 (0.00)	2.9 (0.6)	0.34 (0.08)	0.05 (0.04)	0.01 (0.00)
Lung	0.07 (0.02)	0.01 (0.00)	3.5 (0.6)	0.57 (0.06)	0.05 (0.02)	0.01 (0.00)
Liver	3.7 (1.7)	6.7 (2.9)	0.43 (0.05)	0.65 (0.03)	0.17 (0.14)	0.24 (0.19)
Spleen	0.10 (0.08)	0.01 (0.01)	1.1 (0.2)	0.14 (0.03)	0.11 (0.09)	0.01 (0.01)
Pancreas	0.16 (0.16)	0.04 (0.04)	0.52 (0.20)	0.06 (0.01)	0.25 (0.25)	0.02 (0.03)
Kidney	0.22 (0.04)	0.15 (0.03)	3.5 (0.0)	1.5 (0.2)	0.89 (0.06)	0.35 (0.03)
Muscle	0.11 (0.03)	1.94 (0.58)	0.66 (0.50)	6.4 (4.8)	0.37 (0.32)	3.8 (3.4)
Stomach	0.32 (0.19)	0.38 (0.27)	0.17 (0.02)	0.11 (0.03)	0.12 (0.11)	0.07 (0.06)
Intestine	17.7 (4.0)	60.3 (18.5)	0.37 (0.07)	1.2 (0.2)	0.14 (0.09)	0.44 (0.25)
Bone	0.10 (0.14)	0.43 (0.63)	—	—	—	—
Urine	26.3 (14.1)	—	445.4 (369.2)	—	267.2 (40.9)	—

Data are presented as mean and SD in brackets ($n = 3$).

as the pancreas is surrounded by liver and intestine. The mice used in this study do not develop pancreatic amyloid deposits as rodent IAPP is non-amyloidogenic. Therefore, only background accumulation of radioactivity was seen in pancreas in both biodistribution and imaging studies.

General

All chemicals were obtained commercially and used without further purification. Ethyl 4-(trimethylammonium triflate)benzoate and *N*-succinimidyl-4-fluorobenzoate (SFB) were synthesized as previously reported.[34,35] [(N-Me)G^{24}, (N-Me)I^{26}]hIAPP(22–27) peptide was synthesized by the University of Oklahoma Health Sciences Center (OUHSC) Molecular Biology-Proteomics Facility (Oklahoma City, OK) utilizing traditional Fmoc synthesis strategy. No-carrier-added [^{18}F]F$^-$ was obtained from Midwest Medical Isotopes, Inc. (Oklahoma City, OK). Electrospray mass spectral analysis was performed at the OUHSC Molecular Biology-Proteomics Facility. ^{1}H NMR spectral analysis was performed on a Varian Mercury VX-300 NMR Spectrometer at the University of Oklahoma NMR Facility (Norman, OK). CF-1 (19–21 g) male mice were purchased from Charles River Laboratories International, Inc. (Wilmington, MA). The microPET/CT imaging was conducted in the OUHSC College of Pharmacy Small Animal Imaging Facility (Oklahoma City) using a Flex X-O/X-PET/CT scanner (Gamma Medica-Ideas, Northridge, CA). All animal studies were conducted in accordance with the protocols approved by the OUHSC institutional animal care and use committee.

Reversed-phase HPLC analyses were performed on a Beckman System Gold HPLC equipped with a Beckman Model 126 pump, 166 absorption detector, and a Bioscan Model B-FC-300 radioactivity detector. HPLC solvents consisted of water containing 0.1% trifluoroacetic acid (solvent A) and acetonitrile containing 0.1% trifluoroacetic acid (solvent B). A Sonoma C18 column (ES Industries, West Berlin, NJ) 10 μm, 100 Å, 4.6 × 250 mm) was used with a flow rate of 1.5 mL/min. The HPLC gradient system began with an initial solvent composition of 80% A and 20% B for 2 min followed by a linear gradient to 0% A and 100% B in 15 min, after which the column was re-equilibrated. The UV-absorption detector was set at 254 nm.

Synthesis of FB-[(N-Me)G^{24}, (N-Me)I^{26}]hIAPP(22–27)

A solution of SFB (1.6 mg) dissolved in dimethylsulfoxide (DMSO) (100 μL) and a solution of [(N-Me)G^{24}, (N-Me)I^{26}]hIAPP(22–27) (1.1 mg) dissolved in DMSO (100 μL) and phosphate buffered saline (1 mL) were reacted in presence of triethylamine (10 μL) for 24 h at room temperature. The resultant FB-[(N-Me)G^{24}, (N-Me)I^{26}]hIAPP(22–27) was purified by HPLC and lyophilized to obtain pure product as a white powder. Electrospray MS calculated *m/z* for $C_{39}H_{54}FN_7O_9$: 783.9; found: 782.6 ([M-H]$^-$).

Synthesis of para-fluorohippurate (PFH)

A solution of SFB (12.5 mg, 52.7 μmol) dissolved in dimethylformamide (DMF) (0.5 mL) and a solution of glycine (2 mg, 26.7 μmol) dissolved in DMF (0.5 mL) were reacted in presence of diisopropylethylamine (50 μL) for 18 h at room temperature. The resultant PFH was purified by HPLC and lyophilized to obtain pure product as a white powder (yield 76%, 4 mg). ^{1}H NMR (D_2O, 300 MHz)

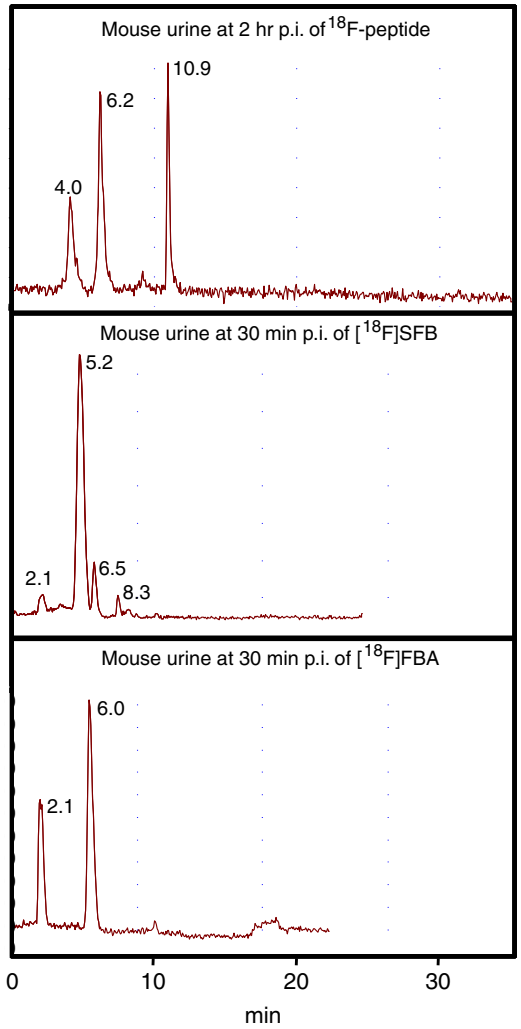

Figure 3. Radio-HPLC chromatograms.

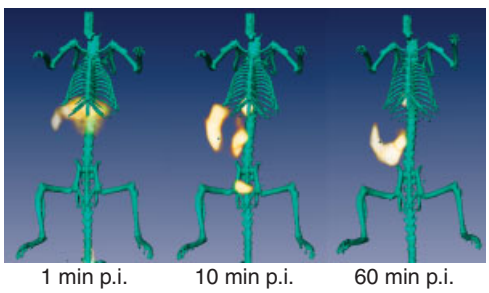

Figure 4. Small animal PET/CT images of a healthy mouse injected with [^{18}F]FB-[(N-Me)G^{24}, (N-Me)I^{26}]hIAPP(22–27).

δ (ppm) 3.99 (s, 2H), 7.09 (m, 2H), 7.70 (m, 2H). Electrospray MS calculated *m/z* for $C_9H_8FNO_3$: 197.2; found: 195.9 ([M-H]$^-$).

Radiosynthesis of *N*-succinimidyl-4-[^{18}F]fluorobenzoate ([^{18}F]SFB)

[^{18}F]SFB was synthesized manually by slight modifications to a previously reported one-pot procedure.[27] [^{18}F]F$^-$ (13.5 mCi) dissolved in water (1 mL) was added to a 5 mL V-shaped bottom vial containing 250 μL of Kryptofix 222 (K222, 20 mg/mL in acetonitrile) and 50 μL of K_2CO_3 (20 mg/mL in water). The solvents were evaporated under a stream of nitrogen at 90°C. Azeotropic drying was repeated with 1.5 mL of acetonitrile to generate anhydrous [K/K222]^{18}F complex.

Ethyl 4-(trimethylammonium triflate)benzoate (5.0 mg) dissolved in anhydrous acetonitrile (1 mL) was added to the dried [K/K222]^{18}F complex and the reaction mixture was heated at 90°C in a sealed vial for 10 min. The resultant ethyl 4-[^{18}F]fluorobenzoate was hydrolyzed to tetrapropylammonium 4-[^{18}F]fluorobenzoate by adding 1M tetrapropylammonium hydroxide (50 μL) and heating the reaction mixture at 90°C in a sealed vial for 5 min. Finally, N,N,N′,N′-tetramethyl-*O*-(*N*-succinimidyl) uronium hexafluorophosphate (12 mg) dissolved in acetonitrile (1 mL) was added and the reaction mixture was heated at 90°C in a sealed vial for 10 min. The reaction mixture was passed through an Oro-Sep SCX cartridge (600 mg, ChromTech), a Sep-Pak® Light Accell Plus QMA cartridge (130 mg, Waters), and a Sep-Pak® Light Alumina N cartridge (130 mg, Waters) connected in series to remove the cationic and anionic organic impurities and unreacted [^{18}F]F$^-$. The cartridges were eluted with an additional 2.5 mL acetonitrile. The solvent was removed under a stream of nitrogen at 90°C. The dried [^{18}F]SFB was redissolved in acetonitrile (100 μL) and injected on to an HPLC column. Pure [^{18}F]SFB fraction was collected and the solvents were removed under a stream of nitrogen at 90°C. The decay-corrected radiochemical yield of the HPLC-purified [^{18}F]SFB was 61.8% EOS. The radiochemical purity of [^{18}F]SFB was >99% as determined by HPLC.

Radiosynthesis of [^{18}F]FB-[(N-Me)G^{24}, (N-Me)I^{26}]hIAPP(22–27) (^{18}F-peptide)

A solution of [(N-Me)G^{24}, (N-Me)I^{26}]hIAPP(22–27) (5 mg) in DMF (25 μL) and triethylamine (10 μL) was added to the dry HPLC-purified [^{18}F]SFB vial and reacted at 90°C in a sealed vial for 35 min. About 50 μL 1M NaOH was added to the reaction mixture to hydrolyze the unreacted [^{18}F]SFB at 90°C for 5 min. The reaction mixture was injected on to an HPLC column and pure ^{18}F-peptide fraction was collected. The solvents were removed under a stream of nitrogen at 90°C. The dried HPLC-purified ^{18}F-peptide was reconstituted in normal saline and passed through a 0.2 μm syringe filter. The decay-corrected radiochemical yield for the HPLC-purified ^{18}F-peptide was 47.6% starting from [^{18}F]SFB. The radiochemical purity of the final product was >99% as determined by HPLC. Total duration of the radiosynthesis starting from [^{18}F]F$^-$ to the injectable ^{18}F-peptide was 253 min.

Radiosynthesis of [^{18}F]fluorobenzoic acid ([^{18}F]FBA)

To a solution of HPLC-purified [^{18}F]SFB in ethanol (100 μL) was added 1M NaOH (50 μL) and allowed to react at 90°C for 5 min. The reaction mixture was neutralized with 1M HCl (50 μL) and diluted with 1.8 mL of normal saline. The solution was passed through a 0.2 μm syringe filter and used for animal studies. The radiochemical purity of the final product was >99% as determined by HPLC.

Biodistribution studies

Three healthy CF-1 mice were anesthetized with 2% vaporized isoflurane and injected with a dose of ~30 μCi of ^{18}F-peptide, [^{18}F]SFB, or [^{18}FFBA in 100 μL normal saline via the tail vein. The mice were euthanized and tissues/organs were excised at 1 h after

injection. The tissues/organs were washed with normal saline, dried by blotting on a tissue paper and transferred to pre-weighed tubes. They were weighed and radioactivity associated with each tissue was recorded on a Packard Cobra II automated gamma counter (PerkinElmer Life And Analytical Sciences, Inc, Waltham, MA). Undiluted standard dose (5 μL) was counted along with the samples. All of the data were corrected for ^{18}F-decay. The percent injected dose (%ID) and %ID/g for each tissue/organ were calculated. The total blood, muscle, and bone mass were estimated as 5.7, 40 and 10% of the total body weight, respectively.[36] The weight of stomach and intestines included their contents.

Small animal PET/CT imaging studies

A CF-1 mouse was anesthetized initially using 2% isoflurane in oxygen at 2 L/min, in a polypropylene induction chamber. When fully anesthetized, the mouse was placed on the scanner bed. Anesthesia was maintained through a nose cone with 1% isoflurane in oxygen at 2 L/min. Body temperature was maintained at $37 \pm 1^{\circ}$C by using a water-circulated pad under the animal. A dose of $\sim$70 μCi of ^{18}F-peptide in 100 μL normal saline was injected into the tail vein. Dynamic small animal PET imaging data were acquired over a period of 60 min after injection. An X-ray computed tomography (CT) was also acquired for 1 min to enable anatomic localization of radioactivity. The PET data were reconstructed using a 2D filtered back-projection algorithm. The PET and CT images were fused together and visualized using Amira 3.1 software (Visage Imaging Inc., San Diego, CA).

Conclusions

The results of this study suggest that [(N-Me)G^{24}, (N-Me)I^{26}] hIAPP(22–27) peptide may not be useful for imaging pancreatic amyloid deposits because of its high accumulation in adjoining abdominal organs. Nevertheless, the study provides a biodistribution of the new class of pancreatic amyloid inhibitors being developed as therapeutic drugs for Type 2 diabetes.

Acknowledgement

This work was funded by the University of Oklahoma College of Pharmacy Startup Grant and Presbyterian Health Foundation Seed Grant C5046801. We gratefully acknowledge the expert technical assistance of Ms Sandra S. Bryant and Mr Kaustuv Sahoo during animal studies. We thank Midwest Medical Isotopes, Inc., Oklahoma City, OK for generously providing [^{18}F]F^{-}.

References

[1] S. E. Kahn, S. Andrikopoulos, C. B. Verchere, *Diabetes* **1999**, *48*, 241.
[2] R. L. Hull, G. T. Westermark, P. Westermark, S. E. Kahn, *J. Clin. Endocrinol. Metab.* **2004**, *89*, 3629.
[3] L. Marzban, K. Park, C. B. Verchere, *Exp. Gerontol.* **2003**, *38*, 347.
[4] A. Lorenzo, B. Razzaboni, G. C. Weir, B. A. Yankner, *Nature* **1994**, *368*, 756.
[5] G. J. Cooper, A. C. Willis, A. Clark, R. C. Turner, R. B. Sim, K. B. Reid, *Proc. Natl. Acad. Sci. U S A* **1987**, *84*, 8628.
[6] A. Clark, G. J. Cooper, C. E. Lewis, J. F. Morris, A. C. Willis, K. B. Reid, R. C. Turner, *Lancet* **1987**, *2*, 231.
[7] P. Westermark, C. Wernstedt, E. Wilander, D. W. Hayden, T. D. O'Brien, K. H. Johnson, *Proc. Natl. Acad. Sci. USA* **1987**, *84*, 3881.
[8] S. E. Kahn, D. A. D'Alessio, M. W. Schwartz, W. Y. Fujimoto, J. W. Ensinck, G. J. Taborsky Jr, D. Porte Jr, *Diabetes* **1990**, *39*, 634.
[9] J. W. M. Hoppener, B. Ahren, C. J. M. Lips, *N. Engl. J. Med.* **2000**, *343*, 411.
[10] R. L. Hull, G. T. Westermark, P. Westermark, S. E. Kahn, *J. Clin. Endocrinol. Metab.* **2004**, *89*, 3629.
[11] J. W. Hoppener, M. G. Nieuwenhuis, T. M. Vroom, B. Ahren, C. J. Lips, *Mol. Cell. Endocrinol.* **2002**, *197*, 205.
[12] A. Clark, M. R. Nilsson, *Diabetologia* **2004**, *47*, 157.
[13] T. A. Mirzabekov, M. C. Lin, B. L. Kagan, *J. Biol. Chem.* **1996**, *271*, 1988.
[14] A. E. Butler, J. Janson, W. C. Soeller, P. C. Butler, *Diabetes* **2003**, *52*, 2304.
[15] M. Bucciantini, E. Giannoni, F. Chiti, F. Baroni, L. Formigli, J. Zurdo, N. Taddei, G. Ramponi, C. M. Dobson, M. Stefani, *Nature* **2002**, *416*, 507.
[16] L. Haataja, T. Gurlo, C. J. Huang, P. C. Butler, *Endocr. Rev.* **2008**, *29*, 303.
[17] P. Westermark, U. Engstrom, K. H. Johnson, G. T. Westermark, C. Betsholtz, *Proc. Natl. Acad. Sci. USA* **1990**, *87*, 5036.
[18] G. G. Glenner, E. D. Eanes, C. A. Wiley, *Biochem. Biophys. Res. Commun.* **1988**, *155*, 608.
[19] K. Tenidis, M. Waldner, J. Bernhagen, W. Fischle, M. Bergmann, M. Weber, M. L. Merkle, W. Voelter, H. Brunner, A. Kapurniotu, *J. Mol. Biol.* **2000**, *295*, 1055.
[20] C. Soto, *Nat. Rev. Neurosci.* **2003**, *4*, 49.
[21] F. E. Cohen, J. W. Kelly, *Nature* **2003**, *426*, 905.
[22] T. Tomiyama, H. Kaneko, K. Kataoka, S. Asano, N. Endo, *Biochem. J.* **1997**, *322*(Pt 3), 859.
[23] L. A. Scrocchi, Y. Chen, S. Waschuk, F. Wang, S. Cheung, A. A. Darabie, J. McLaurin, P. E. Fraser, *J. Mol. Biol.* **2002**, *318*, 697.
[24] A. Kapurniotu, A. Schmauder, K. Tenidis, *J. Mol. Biol.* **2002**, *315*, 339.
[25] M. Tatarek-Nossol, L. M. Yan, A. Schmauder, K. Tenidis, G. Westermark, A. Kapurniotu, *Chem. Biol.* **2005**, *12*, 797.
[26] G. Vaidyanathan, M. R. Zalutsky, *Bioconjug. Chem.* **1994**, *5*, 352.
[27] W. Z. G. Tang, Meixiang Yu, G. Kabalka, *J. Label. Compd. Radiopharm.* **2008**, *51*, 68.
[28] E. Vegt, J. E. van Eerd, A. Eek, W. J. Oyen, J. F. Wetzels, M. de Jong, F. G. Russel, R. Masereeuw, M. Gotthardt, O. C. Boerman, *J. Nucl. Med.* **2008**, *49*, 1506.
[29] C. A. Blackledge, E. A. Partridge, I. D. Wilson, J. K. Nicholson, *J. Pharm. Biomed. Anal.* **2000**, *22*, 1023.
[30] M. Laznicek, A. Laznickova, *J. Pharm. Pharmacol.* **1999**, *51*, 1019.
[31] A. J. Hutt, J. Caldwell, In *Conjugation Reactions in Drug Metabolism* (Ed.: G. J. Mulder), Taylor and Francis Ltd: London, **1990**, p. 273.
[32] G. C. Tremblay, I. A. Qureshi, *Pharmacol. Ther.* **1993**, *60*, 63.
[33] J. Shi, B. Jia, Z. Liu, Z. Yang, Z. Yu, K. Chen, X. Chen, S. Liu, F. Wang, *Bioconjug. Chem.* **2008**, *19*, 1170.
[34] S. Guhlke, H. H. Coenen, G. Stöcklin, *Appl. Radiat. Isotopes* **1994**, *45*, 715.
[35] G. Vaidyanathan, M. R. Zalutsky, *Nat. Protoc.* **2006**, *1*, 1655.
[36] V. D. Awasthi, B. Goins, R. Klipper, W. T. Phillips, *J. Drug Target.* **2002**, *10*, 419.